

GALILEO INFRARED OBSERVATIONS OF JUPITER

T. ENCRENAZ, P. DROSSART, M. ROOS AND E. LELLOUCH
DESPA, Observatoire de Paris
92105 Meudon, France

R. CARLSON, K. BAINES, G. ORTON AND T. MARTIN
Jet Propulsion Laboratory
Pasadena, CA 91109, USA

AND

F. TAYLOR AND P. IRWIN
Department of Atmospheric, Oceanic and Planetary Physics
Oxford University, UK

Abstract.

Galileo infrared observations of Jupiter have been performed with two instruments, the Near Infrared Mapping Spectrometer (NIMS) and the Photo-Polarimeter Radiometer (PPR). A first data set was obtained at the time of the collision of comet Shoemaker-Levy 9 with Jupiter, in July 1994. Information was retrieved about the energy budget of the event, the penetration level of the explosion, the temperature and diameter of the fireball and its evolution with time, the temperature of the atmosphere heated by the infalling debris, and the amount of water formed after the explosion. The second set of data was recorded in 1996 after the Galileo probe entry. Evidence was found for a very low water abundance in the hot spots; this result is in full agreement with the conclusions derived from the Galileo probe. Infrared observations of the Great Red Spot allow to derive its 3-D structure, which appears compatible with the model of an anticyclonic vortex.

1. Introduction

Planetary observations in the infrared spectral range provide an information different from what is retrieved in the visible range. Indeed, the spectrum of

a Solar-system object is characterized by two components: a reflected sunlight component which peaks at visible wavelengths, and a thermal emission which culminates in the infrared range. This thermal emission comes from the part of the solar energy which is absorbed by the planet and reemitted at longer wavelengths; in the case of the giant planets, it also originates from the planets' internal energy. The infrared spectrum of a planet at a given wavelength gives access to its temperature at a specific atmospheric level which depends upon the atmospheric opacity at this wavelength. Thus, infrared observations provide information upon the vertical dimension, in addition to the 2-D images recorded in the visible range.

Infrared thermal sounding of the Jovian atmosphere allows us to probe a wide range of altitudes, from the upper stratosphere (at some near infrared wavelengths) down to the deep troposphere at a pressure of several bars (in the $5\text{-}\mu$ window). In the case of Jupiter, the reflected sunlight component prevails in the continuum at wavelengths shorter than about $4\ \mu$. It gives access to the altitude of the NH_3 cloud, located around 0.5 bar, and provides constraints about the optical properties of the aerosol and cloud particles. In the $3\text{-}4\ \mu\text{m}$ range, where the reflected sunlight continuum is very low (due to a strong methane absorption), thermal emission can be observed at specific wavelengths, in particular in H_3^+ emission lines around $3.5\ \mu\text{m}$, and in the center of the strong ν_3 band of CH_4 at $3.3\ \mu\text{m}$; these observations allow to probe the upper stratosphere, at pressures lower than $1\ \mu\text{bar}$. Above $4\ \mu\text{m}$, a thermal emission continuum increases with wavelength, originating from the troposphere. Indeed, in the $5\ \mu\text{m}$ region, the Jovian atmosphere is transparent to the infrared radiation and deep tropospheric layers are probed, down to a pressure of 5 to 8 bars. Above $7\ \mu\text{m}$, another atmospheric region is probed: this is the 1-0.01 bar region, below and above the tropopause which separates the troposphere from the stratosphere.

Infrared observations of the Jovian atmosphere have been obtained from two instruments of the Galileo orbiter: the Near-Infrared Mapping Spectrometer (NIMS) and the Photo-Polarimeter Radiometer (PPR). Descriptions of these instruments can be found in Carlson et al (1992) and Russell et al (1992) respectively. The NIMS instrument covers the spectral range $0.7\text{-}5.2\ \mu\text{m}$ with a spectral resolution of $0.013\ \mu\text{m}$ below $1\ \mu\text{m}$ and $0.026\ \mu\text{m}$ above. It also has an imaging capability with a pixel size of $0.5\ \text{rnrad}$, which corresponds to a few hundred km on the Jovian disk at the vicinity of perijove during the Jupiter exploration phase (1996-97). The PPR instrument covers a large spectral range ($0.4\text{-}45\ \mu\text{m}$) with a series of discrete filters. Its spatial resolution on Jupiter was about 2800 km at the time of the 1996 observations.

Two sets of infrared data have been recorded on the Jovian atmosphere. The first set was obtained in July 1994, at the time of the collision of comet

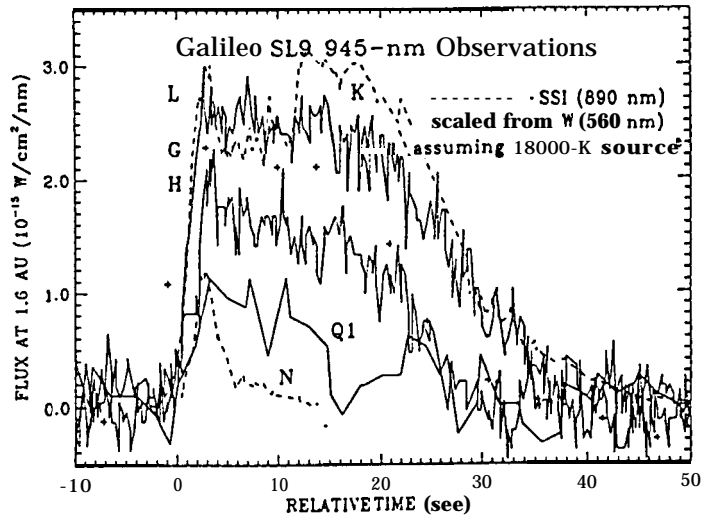


Figure 1. Impact-related lightcurves for the PPR experiment near $0.9 \mu\text{m}$ during the fireball phase of various impacts. These impacts are identified by a letter (L, G, H, etc). Data from the Galileo Solid State Imaging (SS1) system are shown for comparison. The time sequence is remarkably similar for all impacts. The figure is taken from Orton (1995).

Shoemaker-Levy 9 with Jupiter. The comet entered the Jovian atmosphere in a succession of about twenty fragments. Both NIMS and PPR recorded the infrared emissions associated to several of these explosions. The second data set was recorded in 1996, in the months following the entry of the Galileo probe. Special interest was given to the study of hot spots, comparable to the region where the probe entered the atmosphere, and also to the study of the Great Red Spot. In the present paper, we summarize the main scientific results of the two sets of observations.

2. THE SL9-JUPITER COLLISION

The collision of comet Shoemaker-Levy 9 with Jupiter, in July 1994, provided a unique occasion to study in real time the response of a planetary atmosphere to a major meteoritic impact. After its disruption at perijove in July 1992, due to tidal forces, the comet, already split into about 20 fragments, was discovered in March 1993; its collision with Jupiter was predicted at the next perijove passage. The fragments entered the Jovian atmosphere on July 16-22, 1994, at latitude -44 deg., slightly behind the limb; the planet's rotation brought the impact sites into direct view from Earth about ten minutes later. The collision of the fragments resulted in a large variety of phenomena (temperature increase, production of dust and new gaseous species, changes in the magnetosphere)! which were observed

over a wide range of wavelengths, from the ground and from space (HST, Galileo). Reviews of the main observations and results can be found in Nell et al (1996) and Encrenaz and West (1997).

Because of its favorable position with respect to Jupiter at the time of the impacts, Galileo was able to observe the event in direct view. In spite of its large distance from the planet (1.6 AU), the spacecraft was thus able to obtain unique data on the early phase of the phenomenon. Infrared light-curves recorded by Galileo and ground-based telescopes showed evidence for two distinct phases: a “fireball phase” (explosion of the impactor in the Jovian atmosphere and uprising of the fireball) and, about 6 minutes later, a “splash phase” (heating of the atmosphere by the infalling debris). The Galileo data (Fig. 1) were used to provide a reference time scale, and to infer the energy deposition and the temperature (Martin et al, 1995; Orton, 1995; Carlson et al, 1995a,b; Martin and Orton, 1997). Temperatures higher than 10000 K were found at the time of explosion, cooling down to about 2000 K within 16 seconds.

Spectra were recorded with the NIMS instrument, in the fixed-map mode, at the time of the G- and R-impacts. In this configuration, which allows maximum time resolution, the signal is simultaneously recorded on the detectors but the grating is kept fixed. The measurements were then performed at 17 wavelengths separated by $0.28 \mu\text{m}$, with a bandwidth of $0.025 \mu\text{m}$. The spectra were acquired in less than 1 second, and were recorded every 10 seconds. As most of the Jovian disk was included in the NIMS pixel, the signal coming from the impact had to be retrieved from both the reflected sunlight coming from the illuminated part of the disk (toward shorter wavelengths) and the thermal jovian emission (toward longer wavelengths). As a result, the useable part of the NIMS spectra was limited to 10 wavelengths in the 1.8- $4.4 \mu\text{m}$ range, outside which the two cent amination sources are much larger than the impact emission.

Fig. 2 shows a NIMS spectrum recorded during the fireball phase. It basically shows a blackbody continuum, corresponding to a temperature of 2200 K, with absorption bands around 2.3 and 3.5 μm . These bands have been attributed to CH_4 and provide a measurement of the altitude of the fireball. The evolution of the slope of the continuum gives a measurement of the fireball temperature as a function of time. The evolution of the CH_4 absorption with time allows us to follow the ascension of the fireball; the absolute calibration of the spectra provides a determination of its diameter. The fireball was found to expand from about 15 km after 10 seconds to 100 km after 40 seconds (Carlson et al, 1995a,b; 1997). By extrapolating the fireball altitude down to $t = 0$, an estimate of the penetration level can be obtained. In the case of impact G, it corresponds to a pressure level of about 0.2 bar, i.e. above the ammonia cloud (Carlson et al, 1995a). However,

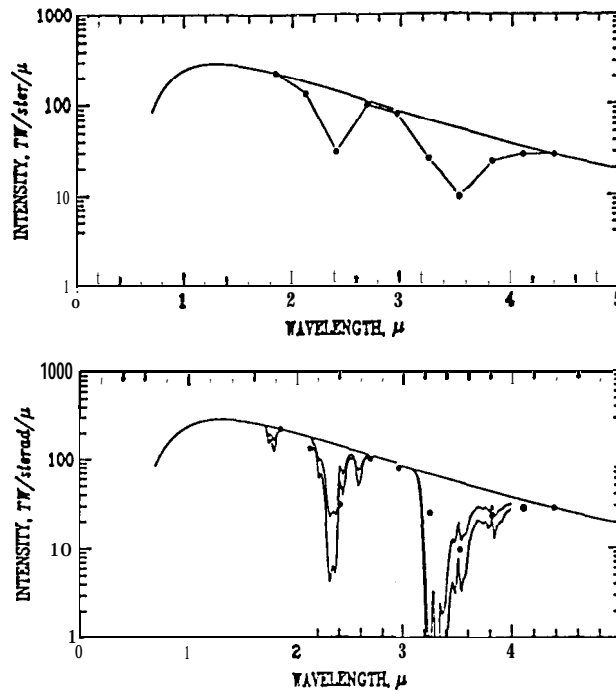


Figure 2. A representative NIMS spectrum of the fireball (top), at the time of G impact (dots), compared to two models (bottom), including CH_4 absorption above 2 pressure levels: 100 mbar (below) and 50 mbar (above). The continuum corresponds to a blackbody emission of 2200 K. The size of the fireball is 40 km. The spectrum is taken 16 seconds after impact. The figure is taken from Carlson et al (1995a).

other observations suggest a deeper penetration level (see Zahnle, 1996, for a review), and the question is not fully solved.

During the splash phase, the shape of the NIMS spectra is completely different, as illustrated in Fig. 3. Two emissions increase with time, one at $2.7 \mu\text{m}$ and the other at $3.5 \mu\text{m}$. The $3.5 \mu\text{m}$ emission is attributed to CH_4 and is an indicator of the temperature of the atmosphere heated by the infalling debris. The $2.7 \mu\text{m}$ emission is attributed to water, newly formed from the oxygen atoms generated in the explosion. These oxygen atoms are most likely of cometary origin, because the atmospheric levels where the Jovian water is present in sufficient abundances appear to be significantly below the penetration level of the colliders. As the temperature is determined from the CH_4 emission, the water emission can be used to retrieve the total H_2O mass. Fig. 4 shows the fit obtained for the last NIMS spectra of the G-sequence, 9 minutes after the impact. For both the G- and R-impacts, the derived temperature is 1000 K. The H_2O mass is about $1.2 \cdot 10^{12} \text{g}$ for the G impact and $2 \cdot 10^{11} \text{g}$ for the R impact (Encrenaz et

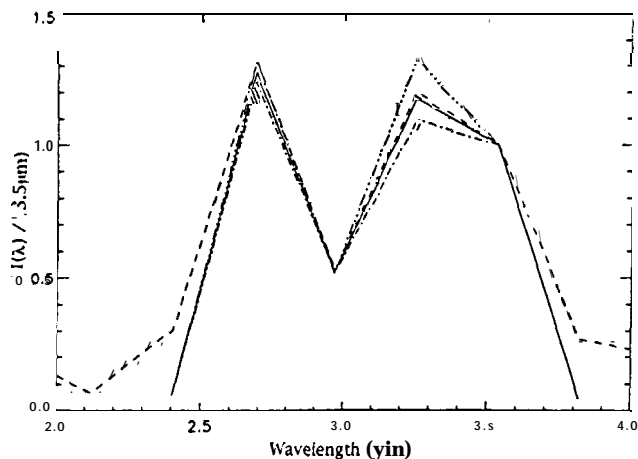


Figure 3. Comparison of the observed NIMS spectrum **9 minutes** after the G-impact, with several synthetic models. Emissions are attributed to H_2O ($2.7 \mu\text{m}$) and CH_4 ($3.5 \mu\text{m}$). The best-fit model corresponds to a temperature of 1000 K and a H_2O mass of $1.2 \cdot 10^3 \text{g}$. The figure is taken from Encrenaz et al (1997).

al, 1997). These numbers are consistent with temperature determinations obtained from ground-based observations (Maillard et al, 1995) and water estimates derived at longer wavelengths from the KAO (Sprague et al, 1996; Bjoraker et al, 1996). With respect to ground-based results, the Galileo data provide a new information about the exact time of water formation; they also provide an upper limit of the production of CO_2 , a molecule which is not observable from the ground.

3. OBSERVATIONS OF THE JOVIAN ATMOSPHERE AFTER THE PROBE ENTRY

Two sets of data have been recorded by the NIMS instrument after the probe entry. First, four “real-time” (RT) spectra were recorded in the vicinity of a hot spot, a region physically similar to the Probe entry site. This hot spot was identified prior to Galileo’s orbital pass using ground-based observations including the 1m telescope at Pic-du-Midi Observatory and the Infra Red Telescope Facility (IRTF) at Mauna Kea Observatory (Orton et al, 1996a). The four NIMS spectra allow us to study the variation of the Jovian atmosphere as one moves from the center of the hot spot to its edge (Carlson et al, 1996). It can be seen that the 5- μm emission is stronger at the center of the hot spot, indicating that the main cloud layer (presumably NH_4SH , at a pressure level of about 1.5 bar) is thinner than

elsewhere.

It is interesting to compare the NIMS RT spectra with a mean spectrum of Jupiter recorded in April 1996 by the 1S0 satellite (Infrared Space Observatory). 1S0, with its 14"x20" aperture centered on the jovian disk, only provides an averaged spectrum, representative of the low jovian latitudes, but has the advantage of a higher spectral resolving power ($R = 1500$). The use of the 1S0 spectrum allows to better retrieve the contribution of the various gaseous absorbers (Encrenaz et al, 1996); the intercomparison of the NIMS data then allows to study their spatial variations. Comparing the NIMS and 1S0 spectra is of special interest in the 5- μ region (Fig. 4), where several gaseous species (PH_3 , GeH_4 , CH_3D , H_2O , NH_3 ...) contribute to the absorption (Roos-Serote et al., 1996). The main result of the 5- μm NIMS study is that the water abundance is very low in the hot spot, in full agreement with the result of the Galileo probe (Niemann et al, 1996). Indeed, a very good fit (Fig. 4a) is obtained with a model using the H_2O distribution derived from the Galileo mass spectrometer experiment: the H_2O abundance is 1% of saturation above the 4-bar level, and 20% of the solar abundance in the 8-11 bar region. The NH_3 abundance used in the 5- μm calculations ($\text{NH}_3/\text{H}_2 = 3.5 \cdot 10^{-6}$ at 0.5 bar, and 1.5 times the solar value below the 3-bar level) is also in agreement with the probe results (Sromovsky et al, 1996; Ragent et al, 1996). The PH_3 and CH_3D mixing ratios used in our model ($\text{PH}_3/\text{H}_2 = 6 \cdot 10^{-7}$; $\text{CH}_3\text{D}/\text{H}_2 = 2.5 \cdot 10^{-7}$) are consistent with previous Voyager measurements (Kunde et al, 1982).

The second NIMS data set ("hot map" or HM spectra) consists in a mapping of a hot spot region, also identified by ground-based observations. Several hundreds of spectra were recorded in the 5- μm region, allowing a determination of the abundances of the tropospheric constituents, and a statistical study of their variations over the disk. This study also confirms that the water abundance is very low in the hot spots. Hotter (i.e. more transparent) regions tend to be associated to the lowest H_2O abundances, which again are consistent with the conclusions of the Galileo Probe. Results of the probe instrument, in particular the nephelometer (Ragent et al., 1996), the Net Flux Radiometer (Sromovsky et al, 1996) and the mass spectrometer (Niemann et al, 1996), indeed suggest that the probe entered a very transparent region, in which the water abundance was strongly undersaturated. It was then suggested (Atreya, 1997) that the region of the probe entry may not have been representative of the whole planet. Convective motions could generate regions of upward motion, cloudy and enriched in condensable gases, and regions of subsidence, clear and dry - the hot spots - similar to the probe entry site. The general circulation of Jupiter seems to associate the cold ascending regions (zones) and the warm subsidence regions (belts); however there is also evidence for structures at much

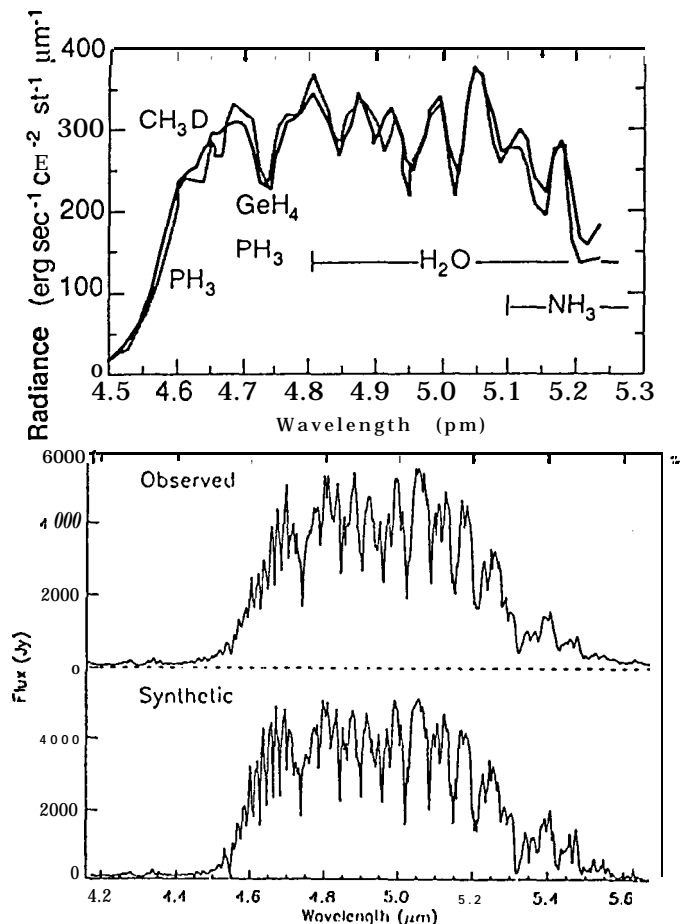


Figure 4. (top) Thermal emission spectrum at the center of the hot spot (same spectrum). The deep troposphere is probed, at pressure levels of 5-8 bars. Absorption are mostly due to PH₃, CH₃D, GeH₄, H₂O and NH₃. (bottom) The mean low-latitude ISO spectrum in the same spectral range. Both data sets are compared with synthetic spectra generated with the same atmospheric model and comparable abundances of the minor species (see text). Our H₂O and NH₃ distributions are consistent with the results of the Galileo probe (Niemann et al, 1996; Sromovsky et al, 1996). The PH₃ and CH₃D mixing ratios are in agreement with the Voyager IR spectra (Kunde et al, 1982). The figure is taken from (top) Carlson et al (1996) and (bottom) Encrenaz et al (1996).

smaller scale, as shown by the high-resolution images and spectra.

In addition to the hot spots, the Great Red Spot was also studied with the infrared instruments of the Galileo orbiter. Images of the GRS obtained with NIMS at several infrared wavelengths (Carlson et al., 1996) show a very rich structure, with part of the feature extending up to a pressure level of 0.24 bar, about 20 km above its base, presumably located at 0.7 bar. A ring of surrounding clouds, higher on the east side than on the west side, is

located a few km below the top level. The Great Red Spot was also mapped by the PPR experiment (Orton et al., 1996b). Observations were recorded at 15, 2225 and 37 μ m. At these wavelengths, the opacity of the atmosphere is mainly due to the collision-induced absorption of hydrogen, involving H₂-H₂ and H₂-He collisions. The penetration level varies between 200 and 700 mbars. Temperature fields were retrieved at two pressure levels: the 250 mbar level (from the 15, 22 and 25 μ m filters) and the 500 mbar level (from the 22 and 37 μ m filters). In the GRS 250-mb map, the coldest temperatures are in the center (111 ± 1 K) and a steep zonal thermal gradient is observed. In the GRS 500-mb map, the minimum temperature, also at the center, is 128 ± 1 K. The PPR observations, in agreement with the NIMS data, show that the GRS is colder with respect to its surrounding. Both NIMS and PPR show that the GRS ring is surrounded by an extended hot spot, wider on the North side. The temperatures and structures observed by NIMS and PPR in the GRS confirm the model of an anticyclonic vortex: the center appears as an upwelling region, with high clouds and adiabatic cooling, and the clear surrounding region seems to be associated with subsidence (Orton et al, 1996b; Gierasch, 1997).

Future infrared observations of Jupiter with the Galileo orbiter will continue at least until the end of 1997. They will allow to study the spatio-temporal evolution of the Jovian atmospheric composition and cloud structure, and should help to provide, in the long term, a better understanding of the Jovian dynamics.

References

- Atreya, S. K. (1997) *Proceedings of the 3G Conference, Padua, January 1997* (this volume).
- Bjoraker, G. L., Stolovy, S. R., Herter, T. L., Gull, G. E. and Pirger, B. E. (1996) Detection of water after the collision of fragments G and K of comet Shoemaker-Levy 9 with Jupiter, *Icarus*, **121**, 411-421.
- Carlson R. W., Weissman, P. R., Smythe, W. D., Mahoney, J. C. and the NIMS Science and Instrumentation Teams (1992), **Near-infrared mapping spectrometer experiment on Galileo**, *Space Sc. Rev.*, **60**, 457-502.
- Carlson R. W., et al. (1995a) Galileo infrared observations of the Shoemaker-Levy 9 G impact fireball: a preliminary report, *Geophys. Res. Letters*, **22**, 1557-1560.
- Carlson, R. W. et al. (1995 b), Some timing and spectral aspects of the G and R collision events as observed by the Galileo Near-Infrared Mapping Spectrometer, *Proceedings of the European SL9-Jupiter Workshop*, R. West and H. Bohnhardt eds, **ESO-CWP52**, 69-74.
- Carlson, R. W. et al. (1996), Near-infrared spectroscopy and spectral mapping of Jupiter and the galilean satellites: results from Galileo's initial orbit, *Science*, **274**, 385-388.
- Carlson, R. W., Drossart, P., Encrenaz, Th., Weissman, P. R., Hui, J. and Segura, M. (1997), *Icarus*, in press.
- Encrenaz, Th. et al. (1996), First results of IS O-SWS observations of Jupiter, *Astron. Astrophys.*, **315**, L397-L400.
- Encrenaz, Th., Drossart, P., Carlson, R. W. and Bjoraker, G. L. (1997), Detection of

- H₂O in the splash phase of G- and R- impacts from NIMS-GALILEO, *Plan. Space Sc.*, in press.
- Encrenaz**, Th. and West, R. M. (1997) The SL9-Jupiter collision: an overview of the Meudon Conference, *Proceedings of the Conference "Asteroids, Comets, Meteors" (ACM96)*, Kluwer, in press.
- Gierasch**, P. G. (1997) Proceedings of the 3G Conference, Padua, January 1997 (this volume).
- Kunde**, V., **Hanel** R. A., **Maguire**, W. C., **Gautier**, D., **Balutau**, J. P., **Marten** A. A., **Chedin** A., **Husson**, N. and **Scott**, N. (1982) The tropospheric gas composition of Jupiter's north equatorial belt (NH₃, PH₃, CH₃D, GeH₄, H₂O) and the Jovian D/H isotopic ratio, *Astrophys. J.*, 263, 443-467.
- Maillard**, J.-P., **Drossart**, P., **Bézar**d, B., de Bergh, C., **Lellouch**, E., **Marten**, A., **Caldwell**, J., **Hilico**, J.-C. and **Atreya**, S. K. (1995) Methane and carbon monoxide infrared emissions observed at the Canada-France-Hawaii Telescope during the collision of comet SL-9 with Jupiter, *Geophys. Res. Letters*, 22, 1573-1576.
- Martin**, T. Z., **Orton**, G. S., **Travis**, L. D., **Tamppari**, L. K. and **Claypool**, I. (1995), Observations of Shoemaker-Levy 9 impacts by the Galileo Photo-Polarimeter Radiometer, *Science*, 208, 1875-1879.
- Nell**, K. S., **Weaver**, H. A. and **Feldman**, P. D. (1996), "The Collision of Comet Shoemaker-Levy 9 with Jupiter", Cambridge Un. Press.
- Orton**, G. S. (1995), Comparison of Galileo SL-9 impact observations, *Proceedings of the European SL9-Jupiter Workshop*, R. West and H. Bohnhardt eds, ESO-CWP52, 75-80.
- Orton**, G. S. et al. (1996a), Earth-based observations of the Galileo Probe Entry Site, *Science*, 272, 839-841.
- Orton**, G. S., **Spencer**, J. R., **Travis**, L. D., **Martin**, T. Z. and **Kamppari**, L. K. (1996b), Galileo Photopolarimeter Radiometer observations of Jupiter and the Galilean satellites, *Science*, 274, 389-391.
- Ragent**, B., **Colburn**, D. S., **Avrin**, P. and **Rages**, K. (1996), Results of the Galileo Probe Nephelometer experiment *Science*, 272, 854-856.
- Roos-Serote**, M., **Drossart**, P., **Encrenaz**, Th., **Carlson**, R. W. and **Baines**, K. H. (1996), First analysis of the Galileo/NIMS spectra of Jupiter in the 5- μ m window, *BAAS*, 28, 1135-1135.
- Russell**, E. E., **Brown**, F. G., **Chandos**, R. A., **Finchey**, W. C., **Kubel**, L. F., **Lacis**, A. A. and **Travis**, L. D. (1992), The Galileo Photo-Polarimeter Radiometer experiment, *Space Sci. Rev.*, 60, 531-563.
- Sprague**, A. L., **Bjoraker**, G. L., **Hunten**, D. M., **Witteborn**, F. C., **Kozlovsky**, R. W. H. and **Wooden**, D. H. (1996), Water brought into Jupiter's atmosphere by fragments R and W of comet Shoemaker-Levy 9, *Icarus*, 121, 30-37.
- Sromovsky**, L. A. et al. (1996), Solar and thermal radiation in Jupiter's atmosphere: initial results of the Galileo Probe Net Flux Radiometer, *Science*, 272, 851-854.
- Zahnle**, K. (1996) Dynamics of the impacts, in "The Collision of Comet Shoemaker-Levy 9 with Jupiter", K. S. Nell et al. eds, Cambridge Un. Press, 183-212.